Journal of Thermal Analysis and Calorimetry, Vol. 90 (2007) 1, 159–165

PHASE DIAGRAMS OF THE KF–K_2TaF_7 AND KF–Ta_2O_5 SYSTEMS

M. Boča[1]*, *V. Danielik*[2], *Z. Ivanová*[1], *E. Mikšíková*[1] *and B. Kubíková*[1]

[1]Institute of Inorganic Chemistry, Slovak Academy of Sciences, Dúbravská cesta 9, 845 36 Bratislava, Slovakia
[2]Department of Inorganic Technology, Faculty of Chemical and Food Technology, Slovak University of Technology
Radlinského 9, 812 37 Bratislava, Slovakia

The phase diagrams of the systems KF–K_2TaF_7 and KF–Ta_2O_5 were determined using the thermal analysis method. The phase diagrams were described by suitable thermodynamic model. In the system KF–K_2TaF_7 eutectic points at x_{KF}=0.716 and t=725.4°C and at x_{KF}=0.214 and t=712.2°C has been calculated. It was suggested that K_2TaF_7 melts incongruently at around 743°C forming two immiscible liquids. The system KF–Ta_2O_5 have been measured up to 8 mol% of Ta_2O_5. The eutectic point was estimated to be at x_{KF}~0.9 and t~816°C. The formation of $KTaO_3$ and $K_3TaO_2F_4$ compounds has been observed in the solidified samples.

Keywords: *miscibility gap, phase diagram, phase transition, tantalum*

Introduction

Tantalum is lustrous, silver-grey metal with high melting point. The high chemical resistance, hardness, malleability and ductility make tantalum suitable for numerous industrial applications (e.g. preparation of equipments working under extreme corrosive conditions, for its absolute resistance to body liquids, tantalum is ideal material for surgery and prosthetics, tantalum is used also in wires for the anode lead as well as for heating elements, shielding, and sintering tray assemblies in anode sintering furnaces...). Tantalum as pure metal can be prepared from its oxide by reduction with Na, Al or C. It can be also electrodeposited from molten fluorides [1–4]. Electrolytic deposition from molten electrolytes is one of the most efficient coating technologies of metal materials. Consequently, it is important to know the physico-chemical properties of the used melts in order to increase the industrial processes efficiency and development of new metal deposition technologies from molten electrolytes. One of the most important characteristics of the used systems is diagram of phase equilibria.

Phase equilibria in the binary system KF–K_2TaF_7 was studied several times [5–10]. The eutectic coordinates and temperatures of fusion of relevant compounds are summarized in Table 1. (Note: In original papers the compositions are given once in mass% once in mol%.)

We are aware of only one phase diagram of the binary system KF–Ta_2O_5 [11, 12]. The system was investigated in the concentration range up to 35 mass% (6.61 mol%) of Ta_2O_5. Eutectic point was reported at 1.80 mass% (0.24 mol%) and 853°C. The formation of crystalline $KTaO_3$ was observed from the melt of this system.

As it can be seen from above, the diversity on data is significant and the revision of the data seems to be important as the investigated system KF–K_2TaF_7–Ta_2O_5 represents one of the possible electrolytes for an alternative process for tantalum production to classical thermal reduction.

Experimental

For the preparation of the samples, the following chemicals were used: KF (Fluka, 99.5%), Ta_2O_5 and K_2TaF_7 (prepared at the Institute of Chemistry and Technology of Rare Elements and Minerals, RAS,

Table 1 Reported eutectic coordinates for the system KF–K_2TaF_7

e_1: x_{KF}/mol%; t_1/°C	$t_{fus}(K_2TaF_7)$/°C	e_2: x_{KF}/mol%; t_2/°C	$t_{fus}(K_3TaF_8)$/°C	Ref.
0.29; 697	–	0.78; 718	776	[5]
0.3; 695	772	0.76; 724	776	[6]
0.215; 717	775	0.745; 727	776	[7, 8]
0.3; 697	730	0.78; 718	780	[9, 10]

---

[*] Author for correspondence: uachboca@savba.sk

1388–6150/$20.00

Akadémiai Kiadó, Budapest, Hungary
Springer, Dordrecht, The Netherlands

Table 2 Measured ($t_{pc,exp}$) and calculated ($t_{pc,calc}$) temperatures of primary crystallization and their differences (Δt) together with eutectic temperatures (t_{eut}) of the system KF–K_2TaF_7

$x_{K_2TaF_7}$	$t_{pc,exp}$/°C	$t_{pc,calc}$/°C	Δt/°C	t_{eut}/°C	Crystallizing phase
0	858	858	–		KF
0.1	811	809.28	1.72	715	KF
0.15	790	789	1	727	KF
0.22	750	759.22	–9.22	724	KF
0.24	736	749.31	–13.31	725	KF
0.25	733	744.16	–11.16	724	KF
0.3	722	733.06	–11.06	722	K_3TaF_8
0.35	742	752.95	–10.95	719	K_3TaF_8
0.4	770	767.06	2.94	720	K_3TaF_8
0.48	778	777.58	0.42	720	K_3TaF_8
0.5	777	778	–1	–	K_3TaF_8
0.52	777	777.59	–0.59	718	K_3TaF_8
0.58	771	771.79	–0.79	717	K_3TaF_8
0.68	754	749.17	4.83	718	K_3TaF_8
0.7	734	743.06	–9.06	717	K_3TaF_8
0.72	733	736.5	–3.5	716	K_3TaF_8
0.75	719	725.89	–6.89	715	K_3TaF_8
0.78	719	714.47	4.53	714	K_2TaF_7
0.8	714	717.55	–3.55	714	K_2TaF_7
0.82	719	724.24	–5.24	712	K_2TaF_7
0.85	733	732.64	0.36	714	K_2TaF_7
0.9	744	742.67	1.33	–	miscibility gap
0.9	749.75	742.67	7.08	–	miscibility gap
0.91	763.95	748.47	15.48	–	miscibility gap
0.92	762.9	752.52	10.38	–	miscibility gap
0.93	767.3	755.93	11.37	–	miscibility gap
0.94	766.95	758.92	8.03	–	miscibility gap
0.95	761	763.4	–2.4	–	miscibility gap
0.95	769.75	763.4	6.35	–	miscibility gap
0.96	758	755.62	2.38	–	miscibility gap
0.97	769.5	770.86	–1.36	–	miscibility gap
0.98	761.45	774.6	–13.15	–	miscibility gap
1	778	782.06	–4.06	–	miscibility gap

Apatite – Russia; min. 99.5%), NaCl (Fluka, 99.5%), KCl (Merck, 99.5%). KF and K_2TaF_7 were dried in vacuum at 130°C for 24 h. Handling of all salts was done in a glove box under dry inert atmosphere.

The temperatures of individual phase transitions were determined by means of thermal analysis method, recording the cooling and heating curves of the investigated mixtures at the rate of 2–3°C min^{-1}. The platinum crucible containing 10 g of the samples was placed into the resistance furnace provided by an Ar atmosphere and adjustable cooling rate. The temperature control and the data processing were performed using a computerized measuring device. The temperature was measured using a Pt–PtRh10 thermocouple calibrated to the melting points of NaCl and KCl. The measured transition temperatures are given in Tables 2 and 3.

X-ray powder patterns of samples were collected on Stoe Stadi P transmission diffractometer equipped with a curved Ge (111) monochromator placed in the primary beam and a linear PSD. In order to achieve a better resolution CoK_α radiation was used. The records were taken in the 2θ range of 7–90° at room temperature each for 6 h.

Table 3 Measured ($t_{pc,exp}$) and calculated ($t_{pc,calc}$) temperatures of primary crystallization and their differences (Δt) together with eutectic temperatures (t_{eut}) of the system KF–Ta_2O_5

$x_{Ta_2O_5}$	$t_{pc,exp}$/°C	$t_{pc,calc}$/°C	Δt/°C	t_{eut}/°C	Crystallizing phase
0	858	858	0		KF
0.001	857.8	857.62	0.18	811.3	KF
0.0015	857.6	857.44	0.16	814.8	KF
0.0025	857.5	857.06	0.44	812.8	KF
0.003	856.45	856.87	–0.42	816.8	KF
0.004	859.4	856.49	2.91	816.2	KF
0.004	858.85	856.49	2.36	815.3	KF
0.005	856.4	856.12	0.28	–	KF
0.006	856.2	855.74	0.46	–	KF
0.0075	854.9	855.17	–0.27	–	KF
0.01	854	854.22	–0.22	–	KF
0.0125	855.45	853.27	2.18	814	KF
0.015	851.1	852.31	–1.21	–	KF
0.0175	852.1	851.35	0.75	811.5	KF
0.0175	851.7	851.35	0.35	814.2	KF
0.02	848	850.38	–2.38	–	KF
0.025	847.7	848.42	–0.72	808.9	KF
0.025	850.2	848.42	1.78	814.8	KF
0.03	847	846.42	0.58	813.7	KF
0.035	844.5	844.38	0.12	814.4	KF
0.04	842.1	842.3	–0.2	813.7	KF
0.04	843.5	842.3	1.2	812.4	KF
0.045	840	840.17	–0.17	813.7	KF
0.05	837.4	837.98	–0.58	814.4	KF
0.055	833.9	835.74	–1.84	814.4	KF
0.06	830.6	833.43	–2.83	815.2	KF
0.065	833.2	830.9	2.3	816.0	KF
0.07	826.9	828.6	–1.7	814.8	KF
0.075	823.7	826.07	–2.37	814.3	KF
0.08	823.35	823.46	–0.11	813.9	KF
0.08	822.25	823.46	–1.21	814.8	KF
0.085	820.5	820.78	–0.28	811.9	KF
0.085	822.7	820.78	1.92	816.0	KF

Theoretical

Thermodynamic models of systems containing complex compounds are usually based on the assumptions of a partial dissociation of these compounds [13]. However, the structure of the present melts is not reliably known. The model presented below is independent on the real structure of the melt.

The model is based on the following assumptions and approximations. The ideal melt contains only ionic pairs of the basic species (in this paper ionic pairs formed from KF and TaF_5) [14]. In the case of the complex compounds present in the solid phase, it is assumed that the compounds completely dissociate to the basic species. Existence of the compounds is included in real behavior of the melt [15].

Let us consider the system AX---BX, in which a compound *k*AX*l*BX exists in the solid-state, where *k*, *l* denote numbers of moles of AX and BX, respectively. In the model we assume that the compound *k*AX*l*BX completely dissociates under melting to the species AX and BX.

It is convenient to change composition of the compound *k*AX*l*BX into compound where

$$p = \frac{k}{k+l},\ q = \frac{l}{k+l} \qquad (1)$$

It is obvious that $p+q=1$. Thus by melting of 1 mole of the compound, which completely dissociates to AX and BX, we will get 1 mol of the melt containing species AX and BX.

The molar enthalpy of fusion of $(AX)_p(BX)_q$ equals to

$$\Delta_{fus}H_m^0[(AX)_p(BX)_q] = \frac{\Delta_{fus}H_m^0(kAXlBX)}{k+l} \qquad (2)$$

The activities of AX and BX are (standard state corresponds to pure component at the temperature and pressure of the melt)

$$a(AX)=x(AX)\cdot\gamma(AX),\ a(BX)=x(BX)\cdot\gamma(BX) \qquad (3)$$

Activity coefficients of AX and BX could be obtained from the molar excess Gibbs energy

$$RT\ln\gamma_i = \left[\frac{\partial(\Sigma n_i \Delta G_i^E)}{\partial n_i}\right]_{T,p,n_{j\neq i}} \qquad (4)$$

Formally, the compound $(AX)_p(BX)_q$ divides the system AX---BX into two subsystems AX---$(AX)_p(BX)_q$ and $(AX)_p(BX)_q$---BX. Then the molar Gibbs energy of a subsystem ΔG_m^* [i.e. AX---$(AX)_p(BX)_q$] is

$$\Delta G_m^* = \Delta G_m - (1-x_i^*)\Delta G_m^0 \qquad (5)$$

where ΔG_m denotes the molar Gibbs energy of the system AX---BX; x_i^* is mole fraction of a component i in the subsystem [i.e. mole fraction AX in the subsystem AX---$(AX)_p(BX)_q$]; ΔG_m^0 denotes the value of the molar Gibbs energy of the system AX---BX at the composition of the pure compound $(AX)_p(BX)_q$. Equation (5) equals to the assumptions that new standard state is chosen for the compound $(AX)_p(BX)_q$. The new standard state means the melt with the composition of the pure compound $(AX)_p(BX)_q$ at the temperature and the pressure of the melt.

When we assume that the chemical potential of the compound $(AX)_p(BX)_q$ corresponding to its standard state is

$$\mu[(AX)_p(BX)_q]=p\mu(AX)+q\mu(BX) \qquad (6)$$

then for the activity of $(AX)_p(BX)_q$ it holds

$$a[(AX)_p(BX)_q]=x[(AX)_p(BX)_q]\gamma[(AX)_p(BX)_q]= \\ = \frac{x(AX)^p x(BX)^q}{x(AX)_0^p x(BX)_0^q}\frac{\gamma(AX)^p\gamma(BX)^q}{\gamma(AX)_0^p\gamma(BX)_0^q} \qquad (7)$$

where $x(i)_0$ and $\gamma(i)_0$ are the mole fractions and activity coefficients of AX and BX in the melt with the composition of the pure compound $(AX)_p(BX)_q$, respectively.

The presented model states an alternative way of the derivation of the same expressions as in [16, 17].

In the binary system the composition dependence of the molar excess Gibbs energy can be described by

$$\Delta G_m^E = x_1x_2(g_0+g_1x_2+g_2x_2^2+g_3x_2^3) \qquad (8)$$

Equation (8) may be divided into the enthalpy and entropy part. Enthalpy part of the Eq. (8) can be also measured directly by calorimetry as it is described in [18].

When miscibility gap occurs in the phase diagram the calculated Gibbs energy of mixing of the system has to be higher than zero within that composition range of this miscibility gap

$$\Delta G_m^{mix} = RT(x_1\ln a_1 + x_2\ln a_2) > 0 \qquad (9)$$

This fact has been taken into calculation of the phase diagram.

Results and discussion

The thermodynamic analysis, i.e. the calculation of the coefficients g_i in the Eq. (8) has been performed using multiple linear regression analysis omitting the statistically non-important terms in the excess molar Gibbs energy of mixing on the 0.95 confidence level according to the Student test. As the optimizing criterion for the best fit between the experimental and calculated temperatures of the primary crystallization the following condition was used for all measured points

$$\sum_n (T_{pc,exp,n} - T_{pc,calc,n})^2 = \min \qquad (10)$$

The values of the enthalpy of fusion of individual components used in the calculations are summarized in Table 4.

Table 4 Enthalpy and temperature of fusion of pure compounds used for the calculation

Component	t_{fus}/°C	$\Delta_{fus}H^0$/kJ mol^{-1}	Ref.
KF	858	28.26	[19]
K_2TaF_7	746	19	
K_3TaF_8	776	52	[20]

System KF–K_2TaF_7

Phase diagram of the system KF–K_2TaF_7 was calculated using the thermodynamic model described above. The model is based on the following assumptions and approximations.

In the first step the composition co-ordinates of the system KF–K_2TaF_7 were transformed to the system KF–TaF_5. This transformation does not reflect the real ionic composition of the melt, but it is suitable to describe the thermodynamic properties. The reason is that the real ionic composition of the melt is not known. Thus it is assumed that compounds existed in the solid-state completely dissociate to the basic species during melting and there is only preferred sorting of the ions based on the coulomb electrostatic interactions in the melt.

The molar excess Gibbs energy of mixing of the system KF–TaF_5 has been expressed by the Eq. (8) and also formation of miscibility gap has been taken into account (Eq. (9)).

The calculated phase diagram of KF–K_2TaF_7 system is shown in Fig. 1. The values of interaction coefficients g_i are given in Table 5. The standard deviation of the approximation is SD=±8.0°C. This relatively high value was increased by considering also the immiscibility region. The standard deviation of the approximation when miscibility gap was not considered has reduced to be SD=±5.2°C.

Table 5 Coefficients g_i of the molar excess Gibbs energy of mixing in the systems KF–K_2TaF_7 and KF–Ta_2O_5

System	Coefficient	g_i/kJ mol^{-1}	SD/kJ mol^{-1}
KF–K_2TaF_7	g_0	–11.2	1.4
	g_1	148.9	20.9
	g_2	–733.2	97.7
	g_3	1844.4	146.4
KF–Ta_2O_5	g_2	114.1	16.5

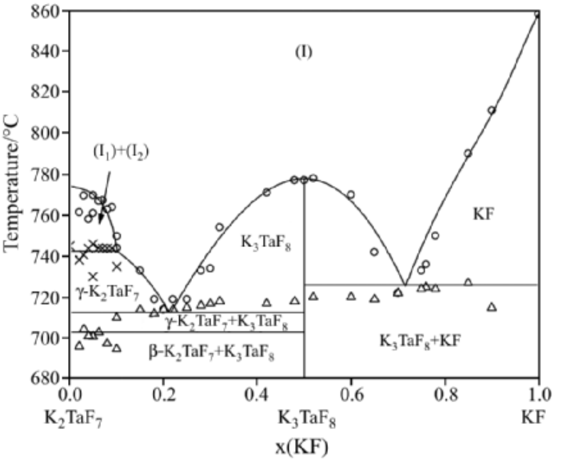

Fig. 1 Phase diagram of the system KF–K_2TaF_7. × – temperature of formation of miscibility gap; full line calculated

On the KF rich side the calculated eutectic point is at x_{KF}=0.716 and t=725.4°C. The composition of this eutectic point is shifted in comparison with other reported data, eutectic temperature corresponds to data reported by [6–8] (Table 1).

The crystallization field of the compound formed from both starting component was observed and according to literature it was attributed to the formation of K_3TaF_8 [5–10]. Temperature of fusion of K_3TaF_8 corresponds reasonably with previously reported data.

On the KF poor side the eutectic point was calculated at x_{KF}=0.214 and t=712.2°C. This result corresponds reasonably to previous data [7, 8]. Coming further from the eutectic point to pure K_2TaF_7 more differences starts to occur in comparison with literature data. It seems that one more solid–solid phase transformation take place around 700°C when β-form of K_2TaF_7 [21] passes to form we have labeled as γ. Moreover, it seems that K_2TaF_7 melts incongruently at cca. 743°C forming two immiscible liquids that mix at 778°C what was previously considered as fusion temperature of K_2TaF_7. The beginning of miscibility gap was estimated at x_{KF}=0.101 at t=742.6°C.

The assumption of miscibility gap comes from the following facts. If partial decomposition of K_2TaF_7 to $KTaF_6$ and K_3TaF_8 would occurred within the first endothermic effect and fusion of K_2TaF_7 within the second one [22], then the material balance of K_2TaF_7 in both processes would be influenced by the kinetics of the process occurring at lower temperature. Longer treatment of the sample at the temperature lower than the beginning of the second process would result in vanishing of the heat effect of the second process at further continuous heating. This was not observed by additional DSC experiment thus the whole initial mass of the sample enters the second process of heating. The beginning of peak of the second heat effect is unexpectedly sharp. This sharpness leads to the assumption that at 746°C (and constant pressure) three phases coexist in the studied system (non-variance equilibrium) and K_2TaF_7 decomposes incongruently into two melts. Moreover, from phase diagrams it is evident that at 730°C K_2TaF_7 cannot coexist with K_3TaF_8 because the K_2TaF_7–K_3TaF_8 system shows around 712°C the eutectic point. (Enthalpy of fusion of K_2TaF_7 at 746°C comes from DSC measurements.)

System KF–Ta_2O_5

The calculated phase diagram of KF–Ta_2O_5 system is shown in Fig. 2. The values of interaction coefficients g_i are given in Table 5. The standard deviation of the approximation is SD=±1.4°C.

The eutectic point based on the calculated data is expected to be at x_{KF}~0.908 and t~816°C. This result is completely different in comparison with reported data [11, 12] where eutectic point was reported at 1.80 mass% Ta_2O_5 (0.24 mol% that corresponds to x_{KF}=0.9976) and 853°C. By our investigation the eutectic point lies at considerably higher Ta_2O_5 concentration. Also eutectic line has been detected at considerable lower temperature. As an example of cooling

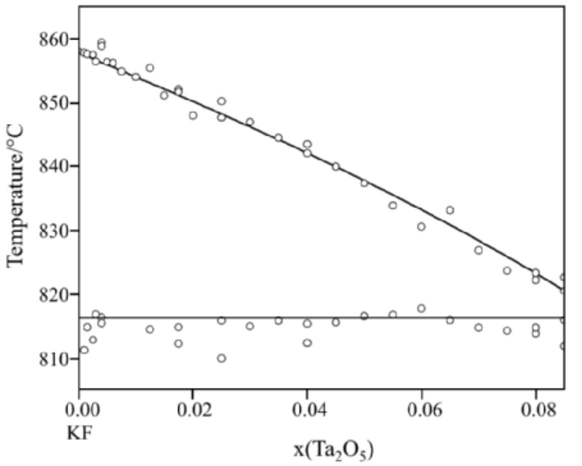

Fig. 2 Phase diagram of the system KF–Ta_2O_5. — – calculated

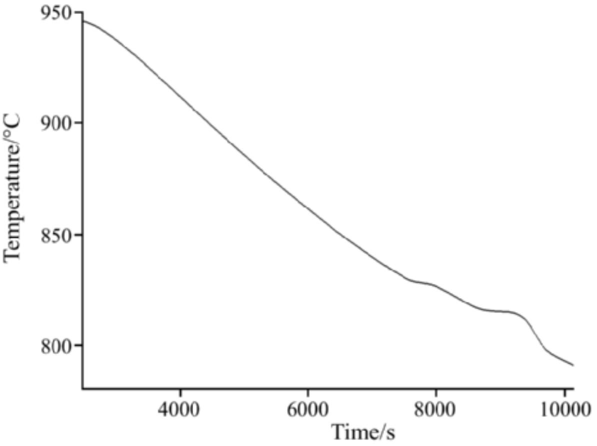

Fig. 3 Cooling curve of the system KF–6 mol% Ta_2O_5

curve the system of 6 mol% was selected clearly showing two thermal effects (Fig. 3), one corresponding to primary crystallization (around 831°C) and second one to eutectic crystallization (around 815°C).

We have spread the investigated region from 6.6 mol% Ta_2O_5 [11, 12] up to 8 mol%. The higher amount of Ta_2O_5 would require longer heating as the mechanism of Ta_2O_5 dissolution in KF seems to be very slow and during this long heating also evaporation is expected in the range that will considerably change the composition thus the analyzing the data would be problematic.

As it was described in [11, 12] we have also detected the presence of $KTaO_3$. Also $K_3TaO_2F_4(s)$ was proved in all samples over 1.5 mol% Ta_2O_5 together with $KTaO_3$ and some other phases (at lower concentration of Ta_2O_5 no other phase as KF was detected because of detection limit does not allow it). It seems that $KTaO_3$ has the lowest solubility and will precipitate as the first one (after KF). It may be caused by significantly higher stability of the above oxotantalate in comparison with oxofluorotantalates. To explain the presence of above mentioned compounds the following reaction scheme can be suggested:

- Melting of KF

$$KF(s)\rightarrow K^+(l)+F^-(l) \qquad (11)$$

- Dissolution of Ta_2O_5

$$\begin{aligned}&K^+(l)+F^-(l)+Ta_2O_5(s)\rightarrow\\&K^+(l)+F^-(l)TaO_2^+(l)+TaO_3^-(l)\end{aligned} \qquad (12)$$

- Mutual reaction of ions; e.g.

$$\begin{aligned}&K^+(l)+F^-(l)TaO_2^+(l)+TaO_3^-(l)\rightarrow\\&K^+(l)+TaO_2F(l \text{ or } g)+TaO_3^-(l)\end{aligned} \qquad (13)$$

- Consequent processes during crystallisation

$$K^+(l)TaO_3^-(l)\rightarrow KTaO_3(s) \qquad (14)$$

- Combination of above reactions (11)–(14) gives

$$KF(l)+Ta_2O_5(s)\rightarrow TaO_2F(g)+KTaO_3(s) \qquad (15)$$

- TaO_2F can undergo further reaction with melted KF

$$TaO_2F(s)+3KF(l)\rightarrow K_3TaO_2F_4(l) \qquad (16)$$

- By combining of reactions (15) and (16) the reaction scheme can be deduced

$$4KF(l)+Ta_2O_5(s)\rightarrow KTaO_3(s)+K_3TaO_2F_4(s) \qquad (17)$$

Mass of the system during experiments has lowered. However, the mass loss was lower than if only TaO_2F would evolve (expected mass loss is 46.4% for Eq. (15)) thus the following equation seems to be combination of reactions (15) and (17).

$$\begin{aligned}&(x+4y)KF(l)+(x+y)Ta_2O_5(s)\rightarrow\\&(x+y)KTaO_3(s)+yK_3TaO_2F_4(s)+xTaO_2F(g)\end{aligned} \qquad (18)$$

To estimate the solubility limit of Ta_2O_5 in KF the following experiments were done. The mixture of KF–20 mol% Ta_2O_5 (Aldrich) was heated at 1000°C for 1 h under dry nitrogen atmosphere in Pt and carbon crucibles. It was expected that Ta_2O_5 will not dissolve completely and residual portion will be possible to detect by XRD. The final sample was powdered and from XRD pattern $KTaO_3$ and $K_3TaO_2F_4$ compounds were indicated as in the case of samples with low content of Ta_2O_5 (1.5–8%). Also compound $K_6Ta_{10.8}O_{30}$ was found what indicate that at higher Ta_2O_5 content also additional reactions take place. Unreacted Ta_2O_5 was identified, as well. It is expected that increasing of the temperature would result in dissolution and consequent reaction of the remaining T_2O_5, as well.

Acknowledgements

Slovak Grant Agencies (VEGA-2/6179/26, APVT-51-008104) and Slovak–French Science and Technology Co-operation for years 2004–2005 under programme Štefánik (number 08 Thermodynamic investigation on the niobium and tantalum based mixtures) are acknowledged for financial support.

References

1 N. N. Greenwood and A. Earnshaw, Chemistry of the Elements, Pergamon Press pls., 1st Ed., Oxford 1984, according: N. N. Greenwood, A. Earnshaw, Chemie prvků, 1st Ed., Informatorium, Praha 1993.
2 Kirk–Othmer, Encyclopedia of Chemical Technology, 4th Ed., Interscience, New York 2001.
3 G. Brauer, Handbook of Preparative Inorganic Chemistry, 2nd Ed., Academic Press, New York 1965.
4 F. Fairbrother, The Chemistry of Niobium and Tantalum, 1st Ed., Elsevier, Amsterdam 1967.
5 T. Iuchi, T. Matsuchima and K. Ono, Bull. Res. Inst. Miner. Press Metall., 15 (1959) 87.
6 T. Iuchi and K. Ono, Sci. Rep. Res. Inst., Ser. A, 13 (1961) 456.
7 P. N. Zuj Bin-Sin, N. P. Luzhnaya and V. I. Konstantinov, Zh. Neorg. Khim., 8 (1963) 389.
8 P. N. Zuj Bin-Sin, N. P. Luzhnaya and V. I. Konstantinov, Russ. J. Inorg. Chem., 8 (1963) 201.
9 D. Efros and M. F. Lantratov, Zh. Prikl. Khim., 37 (1964) 2521.
10 D. Efros and M. F. Lantratov, J. Appl. Chem. USSR, 37 (1964) 2483.
11 P. H. Ts'ui, V. I. Konstantinov, N. P. Luzhnaya, Zh. Neorg. Khim., 8 (1963) 396.
12 P. H. Ts'ui, V. I. Konstantinov, N. P. Luzhnaya, Russ. J. Inorg. Chem., 8 (1963) 204.
13 I. Koštenská and M. Malinovský, Chem. Zvesti, 36 (1982) 159.
14 P. Fellner, J. Gabčová and J. Valtýni, Chem. Papers, 44 (1990) 183.
15 V. Danielik and J. Gabčová, J. Therm. Anal. Cal., 76 (2004) 763.
16 T. Foosnes, T. Østvold and H. Øye, Acta Chem. Scand., A 32 (1978) 973.
17 W. Ch. Bale and A. D. Pelton, Met. Trans., B 14 (1983) 77.
18 C. Paz-Ramos, C. A. Cerdeiriña, J. Troncoso and L. Romaní, J. Therm. Anal. Cal., 83 (2006) 263.
19 M. W. Chase, NIST-JANAF Thermochemical Tables, 4th Ed., Chemical Society; American Institute of Physics for the National Institute of Standards and Technology, 1998.
20 L. Kosa and I. Macková, Thermochim. Acta, 447 (2006) 209.
21 V. Langer, L'. Smrčok and M. Boča, Acta Cryst., E62 (2006) i91.
22 A. I. Agulyansky and V. A. Bessonova, Zh. Prikl. Khim., 56 (1983) 489.

Received: May 25, 2006
Accepted: August 9, 2006

DOI: 10.1007/s10973-006-7700-5